Presentable 23
tech. problem 23
results 22
discussion. 23

91/100

ME 538 Final Report:

Constrained flow past a turbine

Nice report!

12/9/2016

Introduction

A marine turbine was modeled after the one currently in use for experimental testing at University of Washington to simulate the flow field and compute the forces exerted on turbine blades while operating in a flume modeled after the Tyler flume located in the Harris Hydraulics Lab.

Since the swept area of the turbine, with a 0.45-m diameter, consumes 42.4 % of the cross-sectional area of the test section, blockage effects are important to consider when analyzing experimental results. To gain a better understanding of how the high blockage ratio affects the flow field and resulting loading on the blades, simulations of both the turbine with high blockage and relatively low blockage are the focus of this project.

The simulations rely on linear momentum actuator disc theory to model the marine turbine, with virtual discs being an included software feature in STAR-CCM+. Actuator disc theory models a turbine with a disc of cross-sectional area equal in size to the swept area of the turbine blades, with the forces on the turbine distributed uniformly across the frontal area of the disc. Velocity is continuous and uniform over the disc [1]. The force on the frontal area of the disc is related to the pressure drop across the disc by the following equation [1]:

$$F = A(P_1 - P_2), \tag{1}$$

which can be used to determine the estimated output power from the turbine and its power coefficient since power $P = FV$ where V is the velocity across the disc, and the power coefficient is defined by

$$C_p = \frac{P_{turbine}}{\frac{1}{2}\rho A U^3} \tag{2}$$

where U is the free stream velocity, ρ is the density, and A is the swept area of the blades [2]. These parameters are important for comparing the behavior of the turbine model with high and low blockage.

Over winter quarter, additional experiments will be run in the Tyler flume. This project is the first step in developing computational results to compare to experimental results. In the future, more disc models will be developed to simulate the turbine operating at varying pitch angles, which is of particular interest for my research in blade pitch control of marine turbines.

Simulation

To create the virtual disc model in STAR-CCM+, the turbine blades were first modeled in the open-source software Q-blade with the geometry shown in Table 1. The airfoil shapes vary radially along the blade and are defined by NACA 44xx airfoil, meaning a maximum camber of 4% located 40% from the leading edge. The last two digits indicate the maximum thickness as a percentage of the chord. The first four entries in Table 1 were profiled with a circular foil instead of the NACA foil. Qblade uses blade element momentum (BEM) theory to calculate local forces on the blades in order

to generate the thrust and power coefficient tables exported to STAR-CCM+ for the virtual disc model. An image of the resulting blade model is shown in Figure 1.

Table 1. Blade geometry input to Q-blade to create a turbine model.

Radius (m)	Chord (m)	Pre-twist (deg)	Thickness/chord ratio
0.051	0.018	15.40	100.000
0.052	0.018	15.40	100.000
0.053	0.018	15.40	100.000
0.056	0.020	15.40	100.000
0.058	0.024	15.40	86.400
0.061	0.033	15.40	54.400
0.064	0.042	15.40	38.500
0.067	0.044	15.40	28.300
0.071	0.045	15.40	23.600
0.079	0.045	15.27	22.500
0.087	0.043	12.63	21.400
0.096	0.040	10.73	20.200
0.106	0.037	9.36	19.000
0.115	0.034	8.34	17.900
0.125	0.031	7.55	17.200
0.135	0.029	6.92	16.600
0.145	0.027	6.39	15.900
0.154	0.025	5.93	15.300
0.164	0.024	5.51	15.000
0.173	0.024	5.12	15.000
0.181	0.023	4.77	15.000
0.189	0.023	4.44	15.000
0.197	0.023	4.14	15.000
0.203	0.023	3.86	15.000
0.209	0.023	3.62	15.000
0.214	0.023	3.41	15.000
0.218	0.023	3.23	15.000
0.221	0.023	3.10	15.000
0.223	0.023	3.01	15.000
0.225	0.023	2.97	15.000

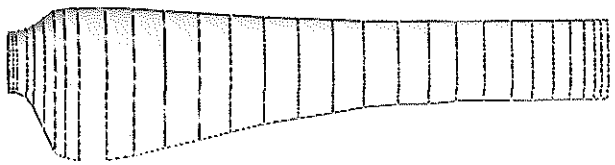

Figure 1. Blade model generated in Qblade using geometry defined in Table 1.

The Reynolds numbers used for the simulation in Qblade were determined from the local chord and radius values [2]:

$$Re = \frac{V_{rel}(r) \cdot c(r)}{\nu} \tag{3}$$

where $V_{rel} = \sqrt{(\omega r)^2 + U_{flume}^2}$, the chord c varies radially across the blade, as listed in Table 1, and ν is the kinematic viscosity of the fluid, and U_{flume} is the free stream velocity of the flow. The Reynolds number at the tip of the blades was calculated to be approximately 94,000, assuming a flume speed of 1 m/s and a rotational rate of 22.2 rad/s which corresponds to a tip speed ratio of 5. Tip speed ratio is defined as

$$TSR = \frac{\omega R}{U_{flume}}.$$

where R is the radius of the turbine, 0.225-m. The power and thrust coefficient tables from Qblade were changed to functions of inflow velocity instead of TSR assuming $\omega = 22.5$ rad/s and a TSR value of 5. These tables were uploaded to STAR-CCM+ using the virtual disc feature and the rotational rate of the disc was set to 22.5 rad/s.

Two computational domains were used for simulations. The first models flow across the turbine in the Tyler flume with high blockage. The blockage ratio is defined by the swept area of the turbine over the cross-sectional area of the channel:

$$\beta = \frac{\pi r^2}{A}$$

For the first simulation, $\beta = 42.4\%$ and the computational domain totaled 1,125,000 cells with dimensions shown in the sketch in Figure 2a. The second simulation used a domain with 4,500,000 cells and a cross-

sectional area of twice the width and height (Figure 2b) and β = 10.6%. Both cases use a cell base size of 0.01.

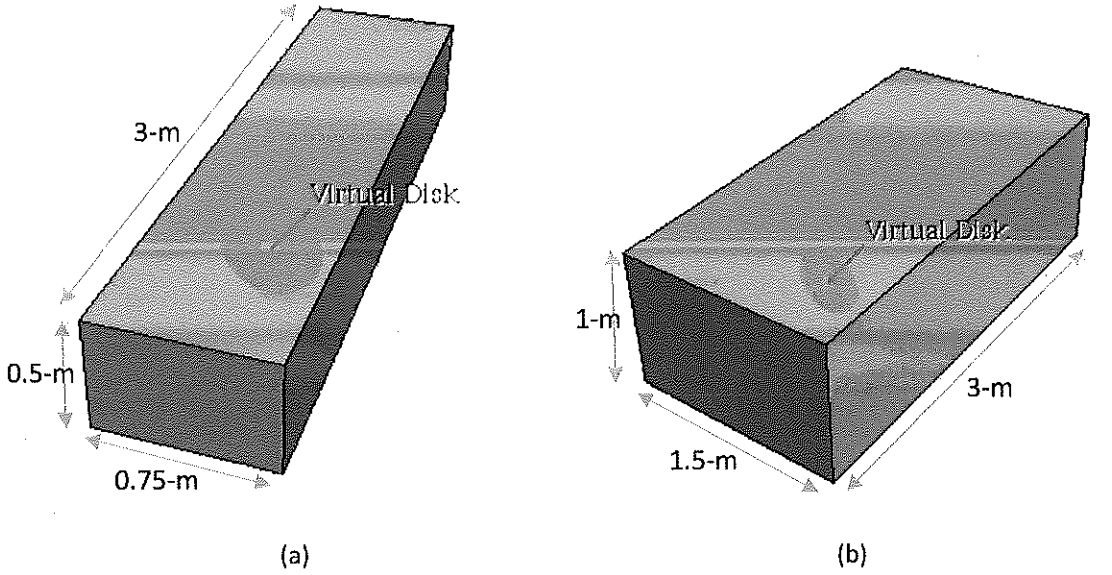

Figure 2. Dimensions of the computational domain for two cases: (a) β = 42.4% and (b) β = 10.6%

The boundary conditions of both domains were chosen to simplify the conditions in the flume. A constant velocity inlet of 1 m/s was used with a constant pressure outlet. Walls with free slip were used for the remaining sides of the domain since modeling the boundary layers are not in the interest of this study. While the actual turbine is in an open channel with a free surface, a rigid lid with free slip was used to simplify the simulation since surface waves are not expected to have a significant effect.

but the behavior of the free surface might have an effect.

Results

Initial observation of the velocity contour plots for β = 42.4% and β = 10.6% shows overall higher velocities for the high blockage case (Figure 3). The fluid in the low blockage case does not have the sharp velocity peaks at the sides of the domain following the disc that it does through the center of the virtual disc, contrary to the case with high blockage. Similar contour plots for pressure show a

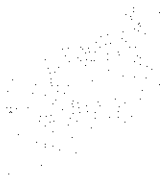

much greater pressure drop across the disc in the high blockage case along with an overall higher pressure build up in front of the turbine due to the constrained flow.

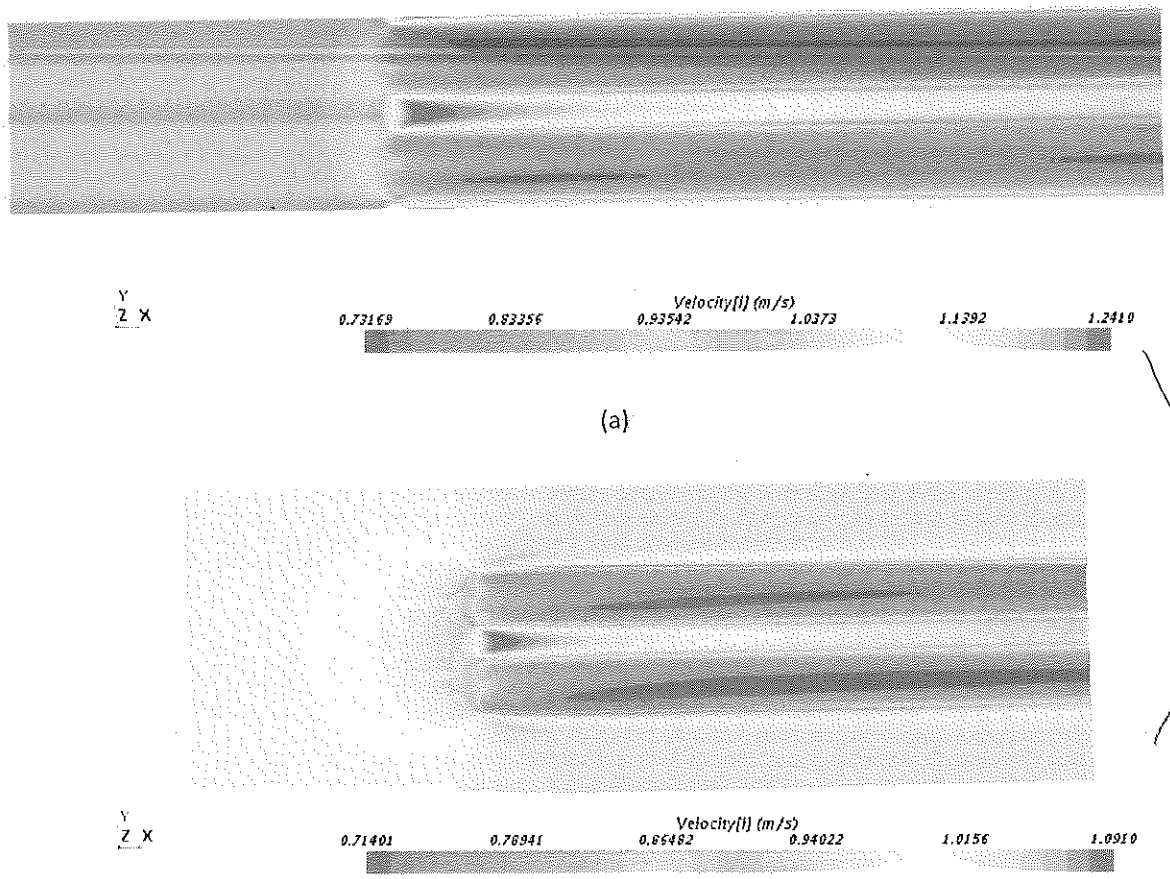

Figure 3. Velocity contour plot for flow past an actuator disc model for (a) 42.4% blockage and (b) 10.6% blockage

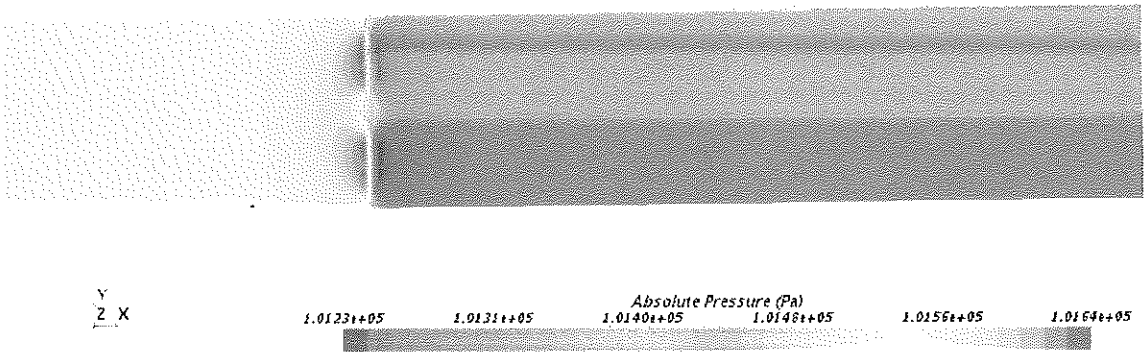

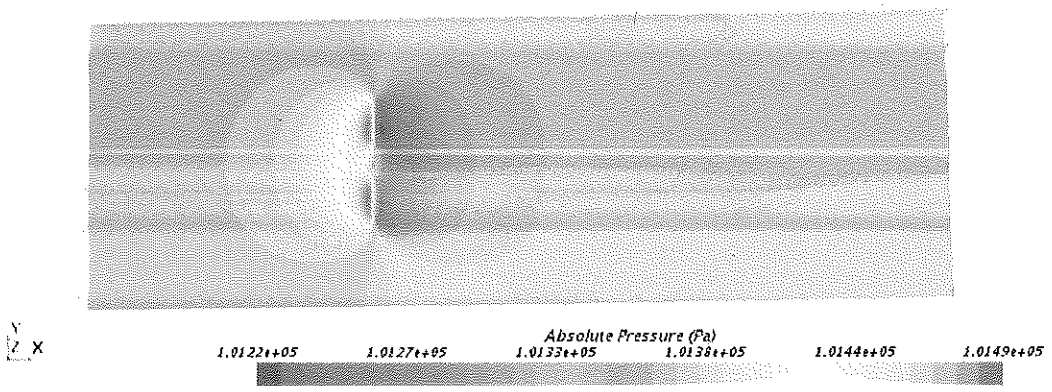

(b)

Figure 4. Pressure contour plots for flow past an actuator disc model for (a) 42.4% blockage and (b) 10.6% blockage

The inflow plane is the cross-sectional plane parallel to the disc from which velocity measurements are used to compute the thrust forces on the virtual disc. The inflow plane was set 10-cm upstream of the disc model, and Figure 5 shows the velocity and pressure profiles across a vertical line in the center of the inflow plane for both high and low blockage cases. As was seen in the contour plots, the high blockage case shows higher velocities and pressure in front of the disc. Velocities near the boundary of the disc are similar in both cases, but in the low blockage case, velocities in the available region beyond the disc are even greater than the inflow velocity. A velocity contour plot of the inflow plane for the high and low blockage cases shows that the velocities remain more uniform in front of the turbine in the low blockage case (Figure 6). Figure 6a shows how the velocity gradients bulge in the y-direction as the constrained fluid has significantly more area to flow pass the turbine on the wider sides of the domain.

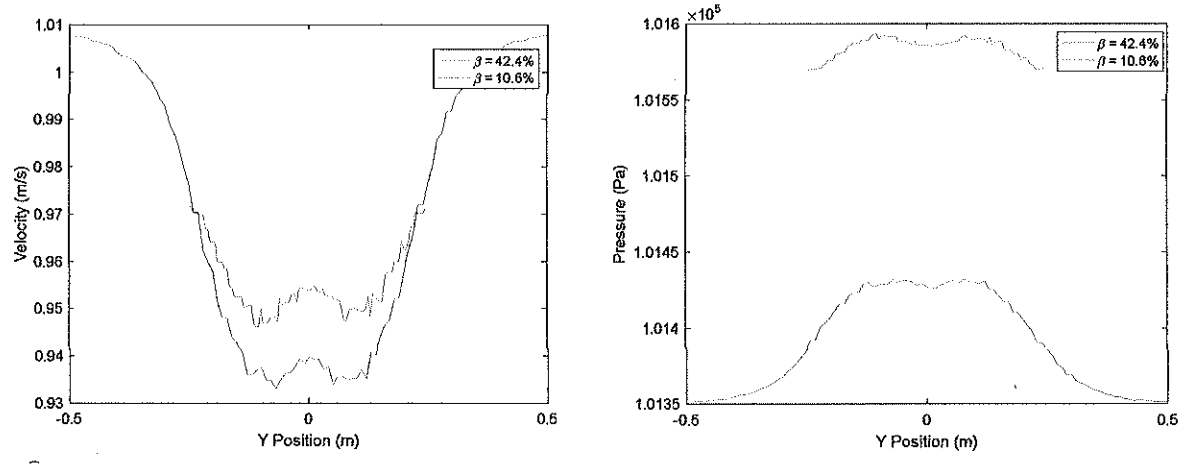

(a) (b)

Figure 5. (a) Velocity and (b) pressure profiles taken vertically across the center of the inflow plane, located 10-cm upstream of the disc model.

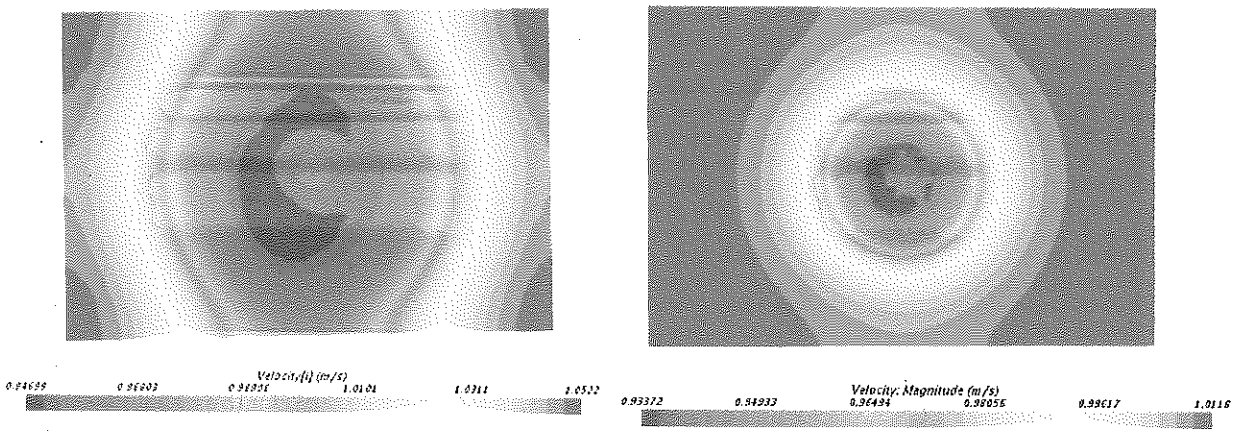

(a) (b)

Figure 6. Velocity contour plots for flow past an actuator disc model at a cross section 10cm upstream of the virtual disc model for (a) β = 42.4% and (b) β = 10.6%

The velocities across the length of the domain, 0.25-m above the centerline, are shown to be larger for the high blockage case (Figure 7a). This profile cross through the center of the "blades" of the turbine model. With limited space around the blades to move the fluid, more flow is forced through the turbine in the high blockage case, resulting in higher velocities downstream of the blades as well. In both cases, we see a velocity decrease in the front of the turbine due to the fluid exerting a force on the actuator disc and a corresponding increase in pressure in front of the disc (Figure 7). The pressure increase is significantly greater for the high blockage case, resulting in greater forces acting on the disc.

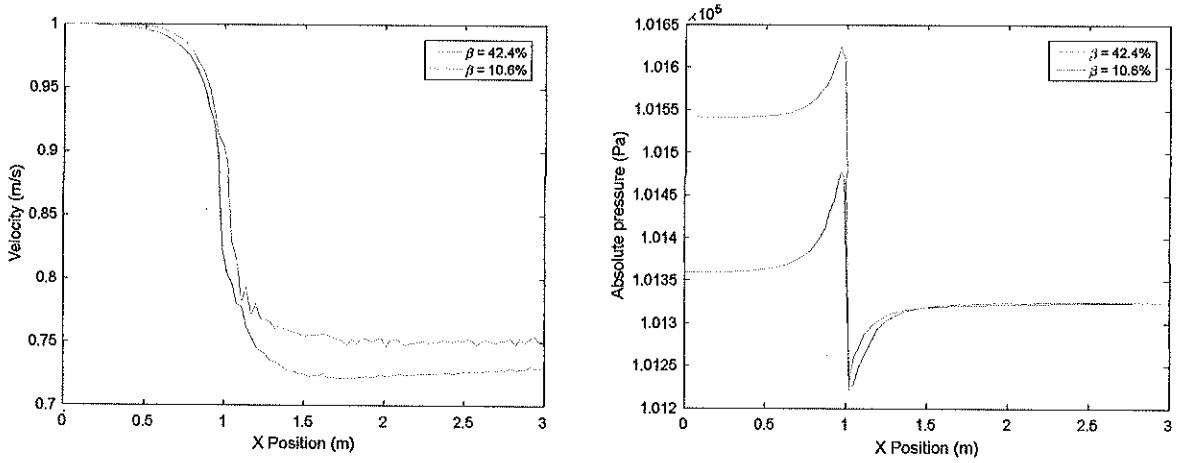

(a) (b)

Figure 7. (a) Velocity and (b) pressure profiles taken across the length of the domain, 0.25-m above the centerline, such that the profile crosses through the center of the blades.

From Figure 7b, the pressure drop in the high and low blockage cases were determined to be 375 Pa and 200 Pa, respectively. Using Equation 1, the axial force acting on the virtual disc was calculated to be 59.6 N for the high blockage case and 31.81 N in the low blockage case. We can get a rough estimate of the power coefficient by observing in Figure 7a that the velocity at the virtual disc is approximately 0.9 m/s and multiplying by the previously determined forces to get an output power of the turbine and using Equation 2 to calculate the available power and resulting power coefficient. This method results in power coefficients of approximately 0.68 for the high blockage case and 0.36 for the low blockage case.

The last observation to make from the simulation is how the downstream velocity profiles maintain their circular shape seen in contour plots in Figure 8. While the inflow plane showed differences in the shape of the contour, both blockage cases show a circular profile one and two diameters downstream of the actuator disc. The effects of the turbine on the flow field remained throughout length of the domain in both simulations.

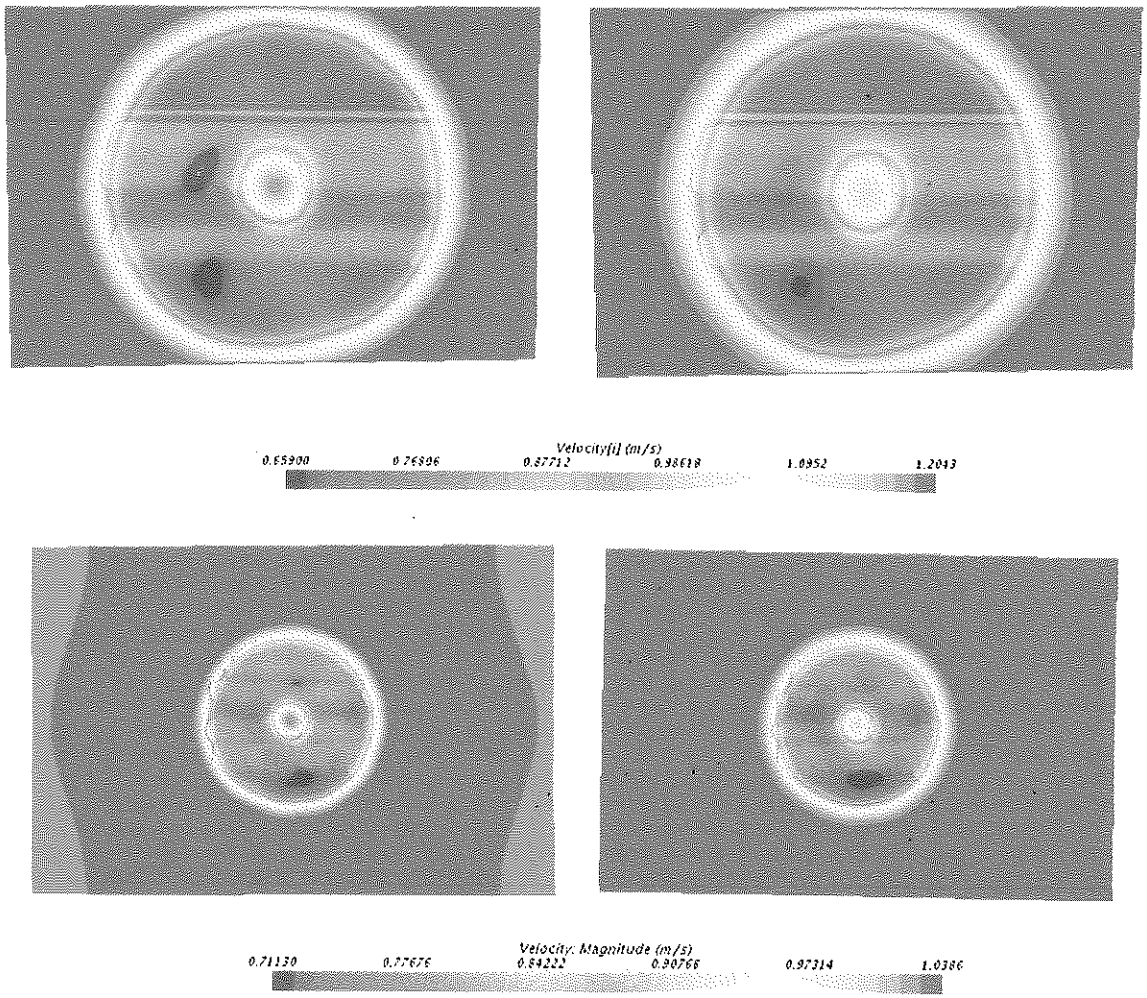

Figure 8. Velocity contour plots for flow past a turbine at a cross section for case β = 42.4% (a) one-diameter downstream and (b) two-diameters downstream of the virtual disc model and equivalent contour plots for case β = 10.6% (c) one-diameter downstream and (d) two-diameters downstream.

Conclusions

The simulations in this study with a turbine in high and low blockage show the significant impact that blockage effects have on the forces and flow field near a turbine. The contour plots and cross section profiles show higher overall velocities in the higher blockage case due to the flow being constrained to the point where flow is forced through the small region of free space near the domain walls or through the hole in the virtual disc, resulting in elevated velocities through these small areas, while excess flow is also forced through the "blades" of the turbine that might typically move around blades. The greater reduction in velocity upstream of the turbine in the high blockage case results in much greater pressures and, thus, a high pressure drop and high force acting on the turbine blades. With forces and power coefficients almost doubled in the high blockage case, it's clear that we should expect significant effects of constrained flow on experimental results, including high forces on the blades and inflated power curves which have already been observed in the flume.

It was also observed that the effects of turbine remain for at least two-diameters downstream of the turbine. Due to the computational and time limits of the project, the domain did not extend far enough beyond the turbine to determine how far downstream we continue to see the effects of the turbine, but this would be an area of interest in future simulations.

Additional future work will include creating virtual disc models for other blade pitches, flume speeds, and rotor speeds. Full performance curves could be generated from simulation to be compared to experimental curves to determine how to correct for blockage or compare to existing blockage correction equations. In future iterations, the mesh should be refined near the surfaces of the virtual disc. Eventually, rotating blade models instead of virtual discs may also be simulated and compared to the actuator disc model.

References

[1] B.L. Polagye. *Hydrodynamic effects of kinetic power extraction by in-stream tidal turbines.* Proquest LLC. 2009.

[2] J. Lassig and J. Colman. *Applied Aerodynamics: Chapter 6 Wind Turbines Aerodynamics.* INTECH. 2014.